P-T-X-fO_2 Conditions in Upper Mantle: Evidence from Lherzolitic Xenoliths Hosted by Plio-Pleistocene Alkali Basalts (Southern Slovakia)

Patrik KONEČNÝ[1], Monika HURAIOVÁ[2] and Miroslav BIELIK[3]

[1] *Geological Survey of Slovak Republic, Mlynská dolina 1, 817 04 Bratislava, Slovak Republic*
[2] *Department of Mineralogy and Petrology, Commenius University, 842 15 Bratislava, Slovak Republic*
[3] *Geophysical Institute of Slovak Academy of Sciences, Dúbravská cesta 9, 842 28 Bratislava, Slovak Republic*

ABSTRACT. Plio-Pleistocene alkali basalts in southern Slovakia in the Cerová Highland ejected upper mantle xenoliths mostly represented by spinel lherzolites, rare harzburgites and dunites. Xenoliths are texturally diverse, including protogranular, porphyroclastic, equigranular, secondary protogranular and secondary porphyroclastic textures showing various stages of deformation and recrystallization in upper mantle. Composition of mineral phases reveals continuous degree of melt extraction. Partial meling event(s) preceded the alkaline volcanism. Highly refractory harzburgites may evolve from the most fertile protogranular xenoliths. Subsolidus temperature is independent of textural types of lherzolites ranging from 850 to 1,050 °C. Oxygen fugacity around FMQ is similar to moderately reduced continental mantle indicating no intensive oxidation corroborated to metasomatism or subduction. P-T stability field of spinel lherzolites is crossed by recent geotherm calculated by 2-D geothermal modelling. The supposed geothermal gradient before 1.9–2.6 Ma should lie above recent geotherm indicating a state of thermal subsidence. Formerly proprosed local mantle diapir was not evaluated by new geophysical research, which indicates rather more complicated structure in the transitional zone between the Pannonian Basin and the Carpathians.

KEY WORDS: spinel lherzolite, xenoliths, Plio-Pleistocene, alkali basalt, southern Slovakia.

Introduction

Late Tertiary to Early Quaternary alkaline volcanism in the Carpathian–Pannonian region is related to extensional tectonic regime, which resulted in upwelling of mantle and thinning of lithosphere (Stegena et al. 1975; Royden 1983; Horváth 1993). Alkaline magma types like alkali bastals, basanites and nephelinites are distributed on the periphery of the Pannonian Basin (Lexa and Konečný 1979). Mantle-derived xenoliths are found in basalts near Graz and Balaton (Kurat et al. 1991; Salters et al. 1988; Embey-Isztin 1989; Szabó and Vaselli 1989; Downes et al. 1992), in the Transylvanian Basin in the Perşani Mts. (Vaselli et al. 1995) and in southern Slovakia–northern Hungary (Hovorka and Fejdi 1987; Kubovics et al. 1988; Huraiová and Konečný 1994, 1995). The aim of this paper is to find relations between textural types of mantle xenoliths and P-T-X-fO_2 conditions derived from mineral assemblages and compare the petrological and geophysical data on matle and lithosphere.

Geological setting

Products of young Neogene to Quaternary alkaline volcanism are distributed on the territory of southern Slovakia and northern Hungary (Fig. 1). Volcanic field is situated on the northern edge of the Pannonian Basin covering an area of about 120 km^2. Alkaline basalts, basanites, tephrites and trachybasalts erupted in Pliocene to Pleistocene between 7.17 and 1.16 Ma. Basaltic volcanism in Southern Slovakia overlies Pliocene sedimentary formations. Xenoliths hosted by alkali basalts are abundant only in a few lava flows. Fresh, unaltered samples have been preferably collected from quarries at localities of Mačacia, Ratka and Fiľakovské Kováče. Xenoliths from Ratka and Fiľakovské Kováče come from different positions in one lava flow. Localities differ also by K/Ar dating of basalts (Balogh, pers. comm.).

Sample descriptions

Most xenoliths belong to Cr-diopsidic group and the rest of them to Al-augite group of lherzolites. Both groups are equivalent to types I and II following the classification of Frey and Prinz (1978). Cr-diopside group is the subject of this study. Mostly green nodules are oval in shape, only few are angular, 1 to 6 cm in size. From 31 collected xenoliths, 23 are lherzolites, 2 dunites and 6 harzburgites. Xenoliths exhibit different textures under polarising microscope. According to the textural classification of Mercier and Nicolas (1975) we have 5 protogranular, 4 porphyroclastic, 6 equigranular, 5 secondary protogranular and 3 secondary porphyroclastic lherzolites. Protogranular ones differ from the others by curvi-linear grain boundaries, large olivines up to 5 mm surrounded by smaller pyroxenes, olivines and spinels up to 1 mm in size. Minerals in porphyroclastic xenoliths are strained and porphyroblasts (~3 mm) are surrounded by neoblastic matrix (<1 mm). Difference in grain size of most porphyroclastic lherzolites is actually not so big as illustrated by Mercier and Nicolas (1975). Equigranular xenoliths contain similarly large grains about 1 mm in size. Reordering of grains in some samples suggests weak foliation (sample Lhz25). The occurrence of spinels in the three mentioned textures is restricted to intergranular spaces. If included in olivines, xenoliths overcome second metamorphic cycle according to the definition of Mercier and Nicolas (1975). A nongenetic term poikilitic is obviously used instead of secondary protogranular or secondary porphyroclastic.

Mineral chemistry

Microprobe chemical analyses of mineral phases were obtained using Jeol-733 Superprobe. Conditions of measurements were set to 15 kV accelerating voltage, 20 nA beam current. Each point was measured for 15–20 s with electron probe focused to approximately 3–5 micrometers. Counts were recast by ZAF correction program. Microprobe was calibrated using both natural and synthetic standards. In every sample at least 5–8 analyses were obtained from each mineral phase. Representative analyses are shown in Table 1.

sample	ol M11	ol Lhz16	ol Lhz20	ol Mr3a	ol Lhz23	opx M11	opx Lhz16	opx Lhz20	opx Mr3a	opx Lhz23	cpx M11	cpx Lhz16	cpx Lhz20	cpx Mr3a	cpx Lhz23	sp M11	sp Lhz16	sp Lhz20	sp Mr3a	sp Lhz23
SiO_2	40.47	40.41	40.83	40.91	40.26	55.25	55.92	55.86	55.06	55.24	51.34	52.09	51.37	52.48	53.43	0.05	0.00	0.12	0.00	0.00
TiO_2	0.05	0.00	0.00	0.00	0.00	0.00	0.08	0.14	0.19	0.06	0.58	0.38	0.61	0.41	0.00	0.09	0.00	0.25	0.26	0.00
Al_2O_3	0.00	0.00	0.04	0.00	0.04	3.79	4.11	3.79	3.29	3.28	6.12	6.21	5.32	4.28	4.5	53.29	54.89	54.06	44.15	48.24
FeO	9.44	9.28	9.69	9.63	8.92	6.53	5.56	6.26	5.86	5.31	2.61	2.49	2.47	3.24	1.64	11.45	11.21	12.2	13.15	11.03
MnO	0.00	0.23	0.22	0.22	0.04	0.17	0.21	0.22	0.09	0.08	0.08	0.06	0.08	0.09	0.07	0.15	0.13	0.07	0.13	0.21
MgO	49.53	49.05	48.97	49.37	50.4	33.18	33.76	33.12	33.87	34.38	15.33	15.48	15.92	16.89	16.19	19.85	20.87	20.5	19.34	18.87
CaO	0.09	0.16	0.12	0.14	0.09	0.71	0.75	0.7	0.8	0.77	21.06	21.01	22.16	19.54	21.6					
Na_2O	0.00	0.00	0.01	0.01	0.05	0.08	0.10	0.00	0.1	0.07	1.55	1.38	0.72	1.16	0.99					
K_2O	0.00	0.00	0.00	0.00	0.00	0.05	0.01	0.00	0.00	0.02	0.00	0.00	0.01	0.00	0.00					
Cr_2O_3	0.11	0.04	0.01	0.00	0.00	0.48	0.28	0.24	0.42	0.52	0.9	0.86	0.62	1.39	0.5	14.73	12.97	13.05	22.68	21.41
Ni	0.35	0.32	0.27	0.00	0.00	0.11	0.13	0.00	0.00	0.00	0.02	0.01	0.17	0.00	0.13	0.39	0.35	0.4	0.18	0.25
Total	100.04	99.5	100.17	100.28	99.8	100.34	100.93	100.33	99.69	99.73	99.61	99.97	99.44	99.49	99.05	100.00	100.42	100.65	99.87	100.03
Cr#																15.64	13.69	13.93	25.63	22.95
Mg#	90.34	90.41	90.01	90.13	90.97	90.06	91.54	90.51	91.16	92.02	91.28	91.71	92.01	90.29	94.62	79.74	81.27	80.00	78.91	80.17

Tab. 1. Representative microprobe analyses of mineral phases in wt.% from lherzolites and harzburgites. Abbreviations: sp – spinel; ol – olivine; opx – orthopyroxene; cpx – clinopyroxene.

Olivine is highly magnesian, containing 89.9 to 92.2 mol.% forsterite component except for sample M21 with Fo content around 87 mol.%. Olivines are mostly unzoned. Olivines from samples with intergranular recrystallization have thin rims depleted in forsterite. Regular substituent for divalent cations is nickel (0.22 to 0.68 wt %). *Orthopyroxene* is also highly magnesian. Mg/(Mg+Fe) ratios range from 89.6 to 93.5. In comparison with coexisting olivines, they regularly contain higher Mg/(Mg+Fe) ratios (about 0.2 to 0.93 mol.%). Al_2O_3 content ranges between 2.36 and 4.89 wt %. Harzburgites are significantly aluminium-depleted, containing around 2.5 wt % Al_2O_3. Cr_2O_3 content ranges from 0.24 to 0.93 wt % and can considerably

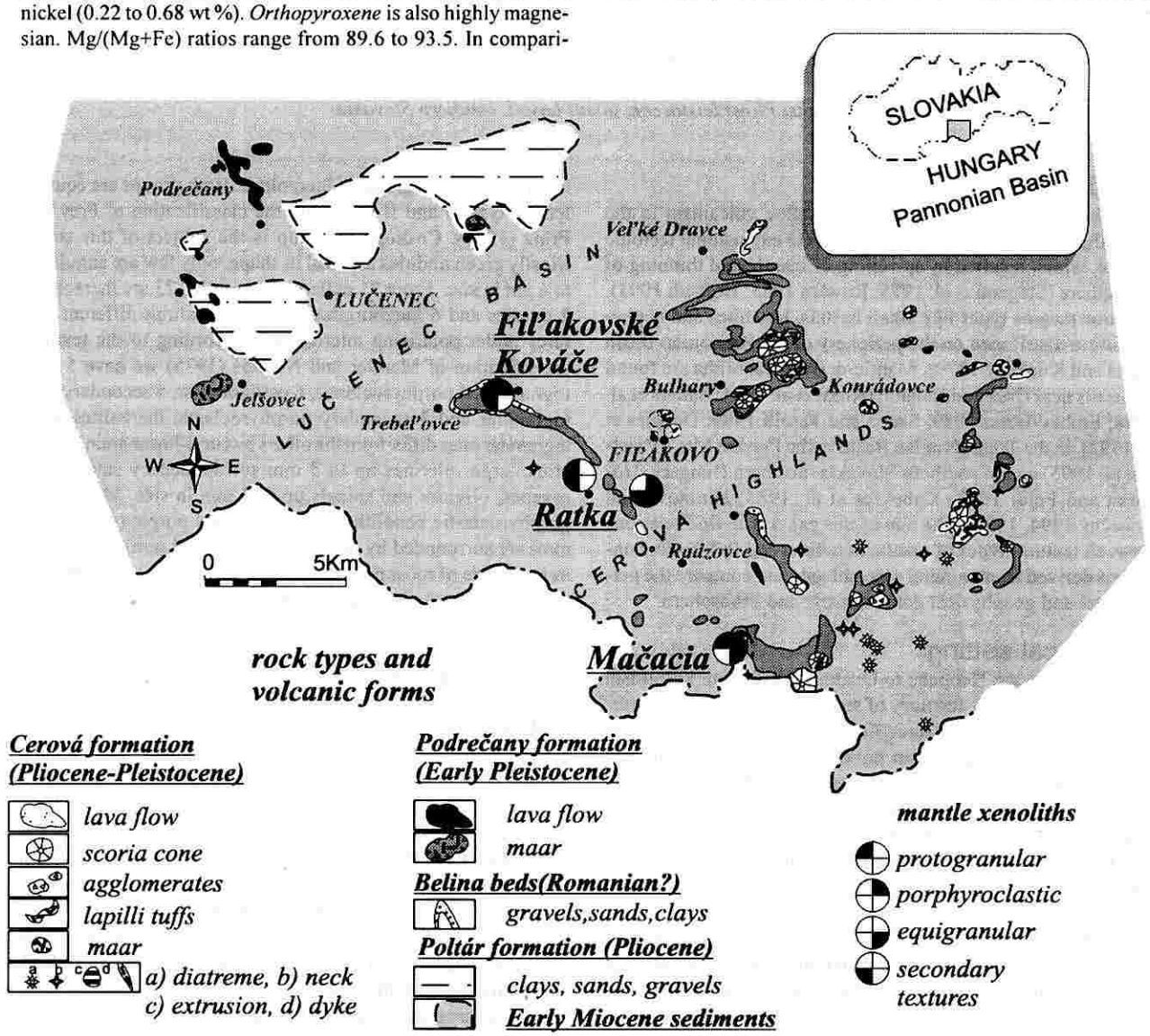

Fig. 1. Geological scheme showing distribution of volcanic forms of Late Cenozoic to Early Miocene alkaline volcanism in southern Slovakia, a northern part of Pannonian Basin. Sampled localities are underlined.

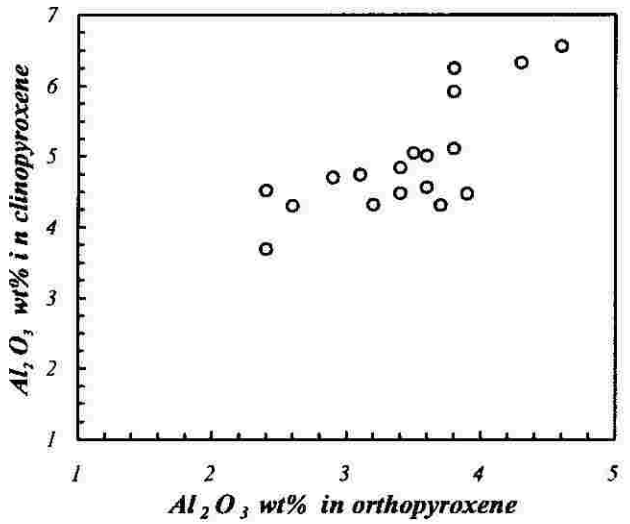

Fig. 2. Positive correlation of Al_2O_3 content in orthopyroxene and clinopyroxene. Data are in Table 2.

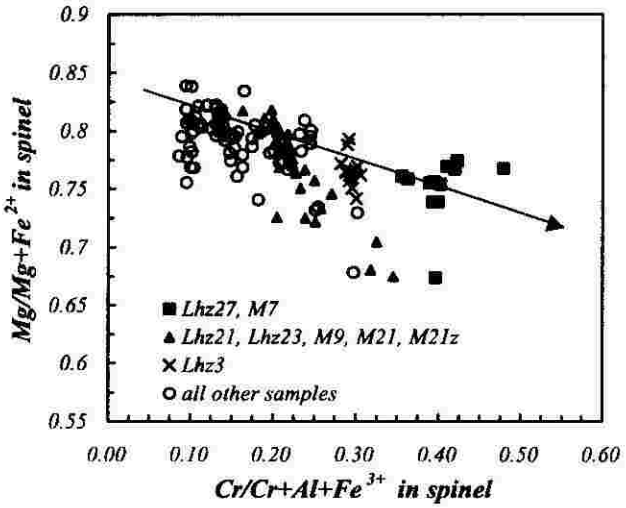

Fig. 3. Depletion related trend in composition of spinels. Re-equilibration to lower temperatures decreases Mg/(Mg+Fe^{2+}) in spinel (Lhz3).

vary in each sample. Samples Mr2 and M11 are depleted in chromium. *Clinopyroxene* belongs to Cr-diopsides, containing 0.39 to 1.91 Cr_2O_3 and 1.63 to 6.85 wt % Al_2O_3 . Al_2O_3 in both ortho- and clinopyroxene correlates positively proving equilibrium coexistence (Fig. 2). Na_2O varies from 0.28 to 1.71 wt % but most clinopyroxenes have more than 1 wt % Na_2O except for Lhz1 and Mr2 (0.4–0.6 wt %). Spinel is classified as Cr-spinel having a variable Cr/(Cr+Al+Fe^{3+}) ratio of 8.6 to 47.9 and Mg/(Mg+Fe) ratio of 66.5 to 82.9. The colour of spinel mostly depends on Cr content, deep brown to black spinels are rich in Cr (M7). Almost all spinels have dark Fe-Cr-rich rim around a lighter core which might form by reaction with host basalt or short- term annealing. Rims have been avoided. Content of ferric iron (15–30 wt % of total Fe) is independent of Cr content. Sieve-like or vermicular spinels are present in samples Lhz4, Lhz8, Lhz20 in contact with fine-grained former melt (?). Spinels are highly chromian and rather equilibrated with the melt than with other minerals. Spinels in Lhz8 partly enclose larger olivine crystals.

Chemical composition of minerals is modified by processes like depletion by melt extraction, low-temperature re-equilibration, reaction with infiltrating melts and/or fluids. Variation in Mg/(Mg+Fe) vs. Cr/(Cr+Al+Fe^{3+}) in spinel defines a negative array (Fig. 3) resulting from coupled substitution of Cr and Fe for Al and Cr during partial melting of average peridotite (Dick and Fisher 1984). Linear correlation is not as good as in orogenic lherzolites (Fig. 3 in Woodland et al. 1992). Vertical dispersion of points is given by decreasing equilibrium temperature (Lhz3). Highly chromian spinels from harzburgites lie at the end of general trend (Lhz27, M7).

An another depletion trend is illustrated in Fig. 4. Metasomatic process tends to increase Cr contents in spinels, while Al contents in orthopyroxenes remain constant. Pyrometasomatism leads to precipitation of sieve-like spinels surrounded by recrystallized fine-grained matrix (Siena and Coltorti 1993). Similar textures are observed in Lhz1 and Lhz8. Only few points plot above the generally defined trend indicating that not metasomatism increased Cr content in spinel but Fe-Cr-rich rims were the most likely analysed. Depletion in olivine and spinel does not continue into the field of subduction-related margins but is confined to the field of oceanic and continental settings. Fo content in olivine increases with Cr/(Cr+Al+Fe^{3+}) – Fig. 5.

Sample Lhz21 plots outside this trend (see below for discussion).

Composition of mineral phases varies with textural types of xenoliths (Table 2). Typical protogranular xenoliths (Lhz22, M11) have Al-rich, Cr-depleted pyroxenes, spinels and forsterite-depleted olivines in accordance with their fertile character. Porphyroclastic xenoliths are similar in composition with protogranular and might originate only as a result of an increase in pressure. Spinels from secondary and equigranular xenoliths are enriched in Cr. Equigranular lherzolites (Lhz20, Mr2) and one secondary porphyroclastic lherzolite (Lhz1) additionally differ in low Na content in clinopyroxenes. Lowering of jadeite componet in clinopyroxene depends on increasing degree of partial melting (temperature) at constant pressure (Walter and Presnall 1993). Harzburgites (Lhz27, M7) are highly refractory. From lherzolites they differ in Mg-rich olivines, low Al content in pyroxenes and by Cr-rich pyroxenes and spinels.

Sample M21 differs from the others in the composition of minerals and in its genesis. Originally secondary protogranular texture is partly replaced by a new mineral generation (about 30 vol %). Newly formed assemblage crystallizes in intergranular spaces and poikilitically encloses older olivines. New spinel has sieve-like shape, new olivines are poor in forsterite, clinopyroxenes are poor in Al and spinels have the lowest Mg/(Mg+Fe) ratio. This sample texturally and mineralogically resembles new melt infiltration, which might metasomatize the older, equilibrated lherzolite. Similar pyrometasomatic textures were reported by Siena and Coltorti (1993).

Thermometry

Many thermometers have been calibrated for lherzolitic systems. The most appropriate and widely used are two pyroxene thermometers based on Al distribution between both pyroxenes (Brey and Köhler 1990), Mg-Fe^{2+} exchange between olivine and spinel (Ballahaus et al. 1991) and distribution of trivalent ions in structural positions of orthopyroxene (Witt-Eickschen and Seck 1991). The thermometers are independent of each other, thus an equilibrium can be corroborated or disproved. Temperatures were calculated at an assumed pressure of 15 kbar because of the lack of a reliable geobarometer for spinel lherzolite assemblages.

Temperatures are consistent regardless of the thermometer

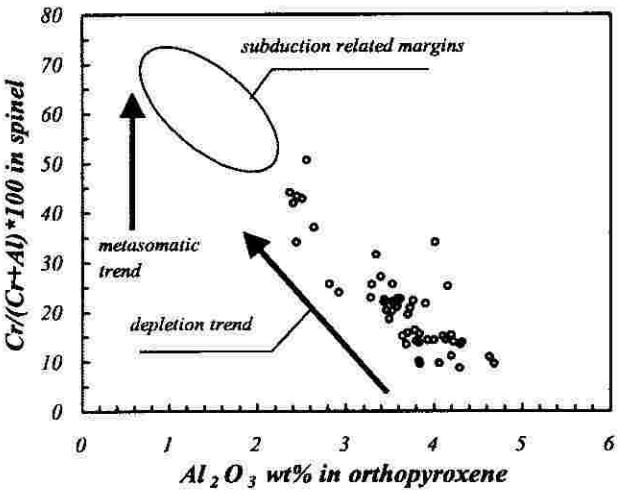

Fig. 4. Cr/(Cr+Al) vs. Al_2O_3 for coexisting spinel and orthopyroxene, respectively. Schematic field for subduction margins reported by Bonatti and Michael (1989).

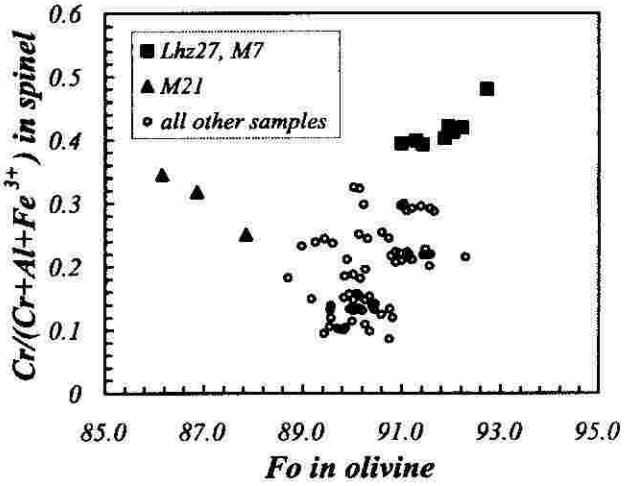

Fig. 5. Variation of Cr/(Cr+Al+Fe^{3+}) in spinel with forsteritic content in coexisting olivine. Sample M21 lies well outside of general trend indicating disequilibrium within sample.

used. Two-pyroxene calibration T_{BKN} yielded temperatures of 850 to 1,050 °C (Table 2). Olivine-spinel thermometer provided temperatures TB systematically lower by about 20–50 °C because Mg–Fe^{2+} exchange between olivine and spinel re-equilibrates to lower temperatures compared to Al–Cr substitution in orthopyroxene. Similar correlation was found in slowly cooled spinel lherzolites beneath Arabian Plate (Medaris and Syada 1998). Orthopyroxene temperature array in Fig. 6 lies between 900–1,000 °C isotherms and is comparable with two-pyroxene thermometry.

Every sample equlibrated in a narrow temperature interval. Concurrently high and low temperatures in samples Lhz22 and M8 indicate local disequilibrium or not finished re-equilibration. Subsolidus temperatures indicate slow cooling and mantle relaxation longer time before the occurrence of alkali magmatism in southern Slovakia.

Oxygen fugacity

Oxygen pressure is an important parameter characterizing conditions in the mantle. Oxygen fugacity depends mostly on ferric iron content in spinel, balanced by oxygen exchange between olivine, orthopyroxene and spinel. Oxygen state has been evaluated utilizing enhanced version of oxygen thermobarometry after Wood and Virgo (1989), Bryndzia and Wood (1990) and calibration of magnetite component in spinel after Nell et al. (1989). The molar fraction of Fe_2O_3 in spinel is considerably low, small deviations introduce large uncertainty in fO_2. To minimize systematic errors we used spinel stadards KLB8316, KLB8315 and MHP79-1 with Fe^{3+} measured by Mössbauer spectroscopy (Table 3 in Wood and Virgo 1989). Calculated fO_2 ranges from -1.56 to +1.23 log units relative to FMQ with average -0.05 log unit. Another oxygen barometer was developed by Ballhaus et al. (1990). This semi-empirical model does not require spinel standards. The range of oxygen fugacity (-2.02 to +0.49, aver. -0.23) is in agreement with fO_2 estimated above, although statistically this model yields values by about 0.4 log units lower than that above (Fig. 7.). Lherzolites from Ratka I and Ratka II seem to be more oxidized if compared to xenoliths from other localities (Table 2).

Increasing oxidation tends to increase the degree of metasomatism in continental lherzolites (Ballhaus 1991). Lherzolites from southern Slovakia are moderately oxidized with no trend towards metasomatized mantle lherzolites (Fig. 8).

Oxidation state can discriminate different geotectonic settings. Continental xenoliths are more oxidized than orogenic or

sample	locality	rock type	texture	ol fo	opx Mg#	opx Al_2O_3	opx Cr_2O_3	cpx Al_2O_3	cpx Cr_2O_3	cpx Na_2O	sp Cr/Cr+Al+Fe^{3+}	sp Mg/Mg+Fe^{2+}	sp Fe^{3+}/Fe	T (°C) TBKN	T (°C) TB	fO_2(FMQ) FB	fO_2(FMQ) FW
Lhz1	Ratka I	lherzolite	sec. porfyroclastic	90.1	91.5	3.7	0.49	4.31	0.69	0.59	17	77.5	23.7	961	895	-0.03	0.45
Lhz2	Ratka I	lherzolite	protogranular	91.1	91.5	3.6	0.4	4.56	1.02	1.03	21.15	77.6	18.9	1048	793	-0.02	0.09
Lhz3	Ratka I	lherzolite	sec. porfyroclastic	91.3	92.4	3.1	0.5	4.74	1.23	1.32	29.4	76.1	19.5	932	850	-0.57	0.33
Lhz16	Macacia	lherzolite	porfyroclastic	90.4	91.6	4.3	0.44	6.33	0.89	1.48	13.5	81.3	21.8	983	793	-0.05	-0.17
Lhz20	Macacia	lherzolite	equigranular	89.4	90.5	3.8	0.33	5.11	0.68	0.78	16.7	80.2	20.1	949	913	-0.3	0.08
Lhz21	Macacia	lherzolite	porfyroclastic	91.3	92.1	3.6	0.46	5.01	0.97	1.28	20.31	79.1	17.6	1086	769	0.02	-0.04
Lhz22	Macacia	lherzolite	protogranular	89.7	90.1	4.6	0.32	6.56	0.64	1.25	9.9	80.5	18.3	1064	813	0.16	-0.61
Lhz23	Ratka II	lherzolite	sec. porfyroclastic	91.3	91.7	3.4	0.5	4.48	0.73	0.95	21.9	77.7	13.5	998	717	-0.84	-0.63
Lhz27	Ratka II	harzburgite	sec. protogranular	91.2	92.2	2.6	0.47	4.3	1.39	1.41	38.4	73.5	22.3	1018	908	-0.54	0.09
Mr2	Ratka II	lherzolite	equigranular	89.7	90.5	3.9	0.28	4.47	0.42	0.39	14.7	79.5	24.9	897	911	-0.12	0.12
Mr3b	Ratka II	lherzolite	sec. protogranular	89.9	92.9	3.4	0.46	4.84	1.45	1.06	28.8	68.4	29.2	1081	1022	0.12	0.59
Mr3a	Ratka II	lherzolite	sec. protogranular	90.4	90.6	3.2	0.48	4.32	1.11	1.12	24.6	76.5	31.3	1003	1083	0.12	0.41
M7	Filakovské Kováce	harzburgite	sec. protogranular	92.2	93.5	2.4	0.52	3.69	1.32	1.18	42.7	76.1	26.5	917	1002	-0.3	0.53
M8	Filakovské Kováce	lherzolite	porfyroclastic	90.2	91.3	3.8	0.32	5.92	0.533	1.17	9.88	77.9	21.9	906	788	-0.26	-0.44
M9	Filakovské Kováce	lherzolite	protogranular	89.0	91	2.9		4.7	0.67	1.05	23.1	75.9	19.8		870	-1.03	-0.4
M11	Filakovské Kováce	lherzolite	protogranular	89.9	91.2	3.8	0.29	6.25	0.87	1.61	15.15	78.6	15.6	926	762	-0.72	-0.9
M21	Filakovské Kováce	harzburgite	sec. protogranular	87.5	89.6	2.4	0.41	4.52	1.09	1.06	26.7	71.4	28.5	1033	1126	-0.48	-0.45
M21z	Filakovské Kováce	lherzolite	protogranular	90.1	92.2	3.5	0.39	5.05	1.2	1.27	23.1	76.1	24.3	1051	937	0.04	-0.2

Tab. 2. Comparison of some chemical parameters of minerals, equilibrium temperatures and oxygen fugacity for lherzolites and harzburgites. Abbreviations: fo forsterite, T_{BKN} temperature after Brey and Köhler (1990), TB temperature after Ballhaus et al. (1991), FB oxygen fugacity after Ballhaus et al. (1990), FW oxygen fugacity after Wood and Virgo (1989), FMQ fayalite–magnetite–quartz oxygen buffer, others in Table 1. Oxygen fugacity expressed relative to FMQ. Data represent averaged values from each sample (>5).

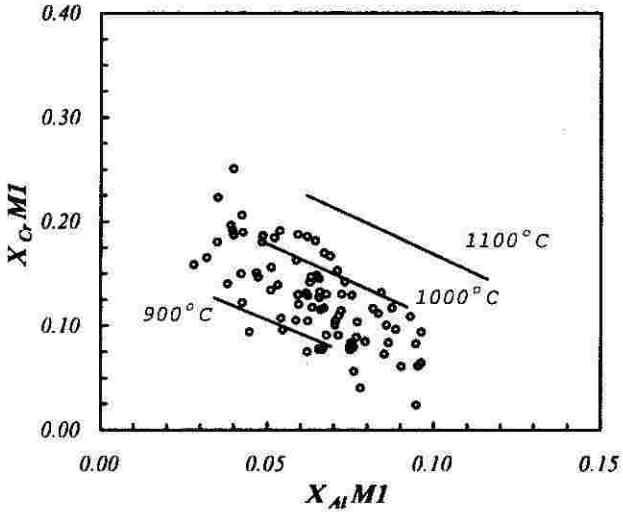

Fig. 6. Temperature dependency of mole fractions of Cr and Al in M1 structural positions in orthopyroxenes. Isotherms from Witt-Eickschen and Seck (1991).

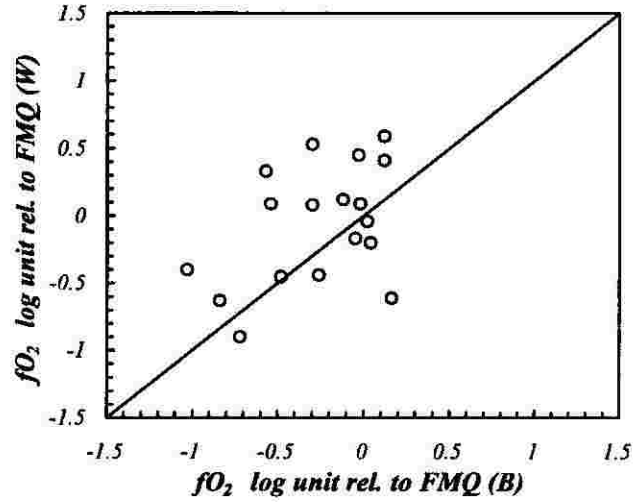

Fig. 7. Comparison of oxygen fugacity calculated from mineral assemblages after Wood and Virgo (1989) (W) and after Ballhaus et al. (1990) (B). Oxygen fugacity, relative to FMQ buffer, calculated at total pressure 15 kbar and at temperatures (T_{BKN}) obtained by the two-pyroxene termometry after Brey and Köhler (1990). Data used are in Table 2.

abyssal peridotites (Wood and Virgo 1989; Woodland et al. 1992; Bryndzia and Wood 1990). Typical continental mantle has majority of fO_2 estimations above FMQ (Bryndzia and Wood 1990, their fig.4). Oxidation of lherzolites from S Slovakia with most fugacity estimations scattered below FMQ resembles a relatively reduced continental mantle (e.g. Kilbourn Hole, San Carlos) with affinity to small Pyrenean orogenic massifs. Metasomatism appears to be coupled with oxidation. Hydrous lherzolites are relatively highly oxidixed with fO_2 more than +0.5 log unit above FMQ. The studied samples do not contain amphibole, which implies that no strong metasomatic changes occurred in upper mantle beneath southern Slovakia. Oxygen fugacities estimated for different textural types of lherzolites overlap. Perharps secondary protogranular xenoliths are more oxidized than secondary porphyroclastic ones. Less oxidized below FMQ are harzburgites.

Recent geophysical features on lithosphere

It is necessary to understand the area of southern Slovakia in the context of Pannonian Basin in the south and Central Western Carpathians in the north.

The studied area is characterized by thickening of *Moho* towards north. On the Hungarian–Slovak state boundary Moho can be observed at a depth of 27.5 km and in Veľké Dravce at a depth of 30 km (Horváth 1993; Šefara et al. 1996). Maximum elevation of about 25 km lies in the vicinity of Debrecen (Hungary). Based on available seismic data no local elevation exists in the region of S Slovakia.

Lithospheric thickness follows Moho. A significant elevation of *asthenosphere* (60 km) extends across the eastern margin of the Pannonian Basin and thickening towards north, under the Carpathians. Astenosphere is relatively thin beneath S Slovakia, only about 70 km.

Neither seismically (Babuška et al. 1988; Horváth 1993) nor geothermally defined (Majcin et al. 1998) lithosphere/asthenosphere boundary does create any local elevation.

Density of *surface heat flow* is ca. 80 mWm^{-2} (Majcin et al. 1998; Lankreijer 1999). Maximum anomaly (100 mWm^{-2}) is located in the Bükk–Mátra Mts. (Šefara et al. 1996). Extrapolated temperature at Moho lies around 900 °C (Majcin et al. 1998).

Southern Slovakia is characterized by significant *gravity* anomaly with amplitude of +20 mGal, located around Kostná dolina (Gemerský Jablonec) (Šefara et al. 1987; Szalaiová and Šantavý 1997). Gravity anomaly has been interpreted by different methods (Bodnár and Pospíšil 1987; Grecula and Varga 1979; Fusán et al. 1987) but is generally explained in context of basaltic volcanism.

Magnetic field in the given area forms a local anomaly of max. 400 nT (Šefara et al. 1987). Questionable is the depth of the anomaly.

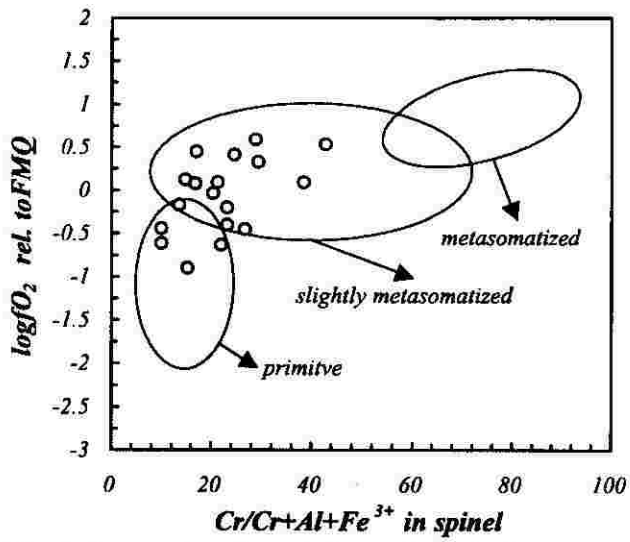

Fig. 8. Oxygen fugacity, relative to FMQ buffer, vs. Cr/(Cr+Al+Fe^{3+}) (spinel). Fields of primitive to metasomatized xenoliths given by Ballhaus et al. (1990). Data are in Table 2.

The *rheological* study of lithosphere (Lankreijer et al. 1999) and rheological profile 2T which estimates strenght of lithosphere against stress in compressional regime implies that:

- uppermost part of the upper crust is characterized by one rheologically harder layer of small thickness at a depth of ca. 3–8 km.
- lower crust up to lower lithosphere is weak, resulting from temperature increase and abrupt deeping of asthenosphere towards the north.

Discussion

Upper mantle in soutern Slovakia is represented by spinel lherzolites, less abundant are harzburgites and dunites. P-T-X-fO_2 data are consistent within each sample (except for M21) implying good re-equilibration. Depletion in mantle controls bulk rock chemistry and hence composition of mineral phases. Partial melting in upper mantle is proved by linear depletion trends of mineral composition. The age of the depletion is unknown. Provided that the lherzolitic nodules are well equilibrated and represented pieces of upper mantle at 1.9–2.6 Ma, the depletion process might be older than the Pliocene. Among the collected samples, most fertile is lherzolite M11 with protogranular texture. The most refractory residuum after melting is represented by harzburgites Lhz27, M7.

Primary fluid inclusions in olivines and pyroxenes are CO_2-rich with minor CO and N_2 (Huraiová et al. 1991; Huraiová and Konečný 1994). As a model of melting the system peridotite + CO_2 can be accepted. At 15 kbar, incipient melting starts at temperature of about 1400 °C and at 30 kbar first melt fracion appears at ~1200 °C (Wendlandt and Mysen 1980). Nodules from southern Slovakia equilibrated at 900–1080 °C representing subsolidus temperatures and also incapability of melting. Agents decreasing solidus temperature like amphibole and phlogopite were not observed in studied samples. Increasing degree of partial melt (Xmelt) tends to increase Mg/(Mg+Fe) of olivine and orthopyroxene. Up to 20% degree of partial melting orthopyroxenes have higher Mg/(Mg+Fe) ratio than olivines (Wendlandt and Mysen 1980). The same relation is valid for lherzolites from southern Slovakia suggesting low degree of partial melting.

Change in pressure is buffered by Ca exchange between olivine and clinopyroxene and was used for calibration of geobarometer (Köhler a Brey 1990). P-T array obtained by combination of T_{BKN} and P_{BKN} gives unrealistic field extending from 8 to 30 kbar (Fig. 10). Despite the lack of reliable barometer for spinel lherzolites, the pressure extent is confined between Moho and spinel/garnet phase transition. Phase boundary shifts according to Cr content of spinel which increases the stability field of spinel at higher pressures. Pressure stability field is assesed to be 9 kbar to 15 kbar for less chromian spinels or 25 kbar for Cr-rich spinels. The densest primary CO_2 inclusions (0.99 gcm^{-3}) from pyroxenes formed at pressures of about 10.3 kbar correspond to a depth of about 30 km, suggesting mostly upper mantle origin (Huraiová and Konečný 1994). Geophysically modelled geothermal gradient with density of surface heat flow about 80 mWm^{-2} crosses Moho at temperature of 800 °C (Fig. 10). The lowest equilibrium temperatures derived from mineral assemblages are by ca. 100 °C higher. Provided that the samples represent termal state before 1.9–2.1 Ma and thermal subsidence in southern Slovakia, we may speculate about a higher heat flow of ~90–100 mWm^{-2}, typical of provinces of active alkaline volcanism (e.g., O'Reilly and Griffin 1984). The stage of re-equilibration of lherzolites toward lower temperatures subsequently with thermal event(s) is documented by well-developed exsolution lamellae in pyroxenes.

Genetic link exists between textural types of lherzolites and small diapiric structures in the uppermost mantle well known from Massif Central (France) (Nicolas et al. 1987; Witt-Eick-

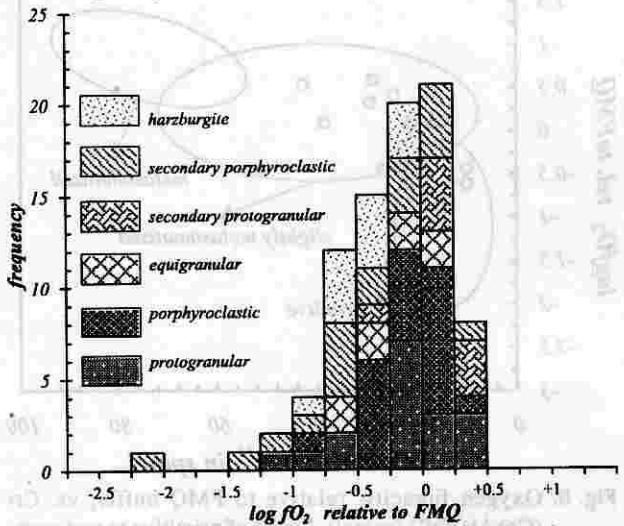

Fig. 9. Oxygen fugacity vs textural types of lherzolites and harzburgites. Data on oxygen fugacity, relative to FMQ buffer, calculated after calibration of Ballhaus et al. (1991).

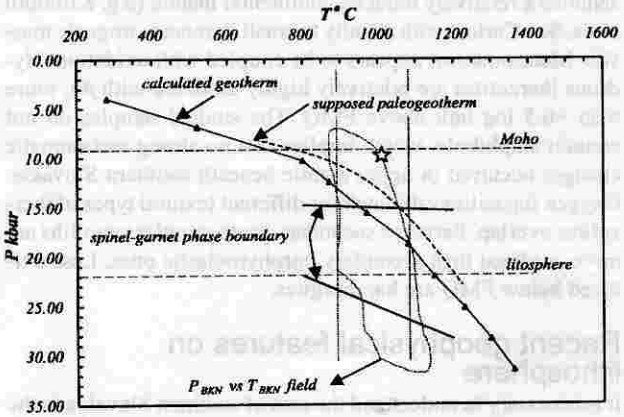

Fig. 10. Estimation of P-T condition for upper mantle lherzolites. Dashed vertical lines mark temperature range (T_{BKN} in Table 2). Upper pressure limits Moho ~27 km and lower pressure depends on spinel/garnet phase transition. Upper solid line obtained for spinel with Cr/(Cr+Al) = 8.8 and lower solid line with Cr# = 50.7, following equations from Webb and Wood (1986). A star indicates pressure from the densest primary CO_2 inclusions (Huraiová and Konečný 1994). Geotherm inferred from geophysical measurements (triangles connected by solid lines) transects the field of spinel lherzolite stability. According to temperature of about 900°C at Moho and temperature derived from mineral assemblages (T_{BKN} in Table 2) we may speculate about higher P-T gradient of supposed peleogeotherm, shown as dashed curve. The P-T estimations after Köhler and Brey (1990) (P_{BKN} vs. T_{BKN}) illustrate uselessness of pressure data due to low temperature re-equilibration and/or limitation of microprobe to detect low Ca content in olivine on the order less than 0.01 wt.%.

schen 1993). Deformed xenoliths are distributed along diapir margins, surrounding undeformed xenoliths in the central part. A similar diapir has been supposed in southern Slovakia (Huraiová and Konečný 1994). New geophysical and mineralogical results do not corroborate its existence. The study area is located at the border between the Pannonian Basin and Central Western Carpathians. This transitional zone, characterized by thickening of Moho and asthenospere to the north, higher density of surface heat flow, gravity and magnetic anomaly, has a complicated origin. Low effective elastic thickness in the lithosphere might facilitate the ascent of basaltic magma.

Conclusions

Upper mantle of southern Slovakia in the Cerová Highlands (northern edge of Pannonian Basin) is depleted to various degrees. The trends of depletion between mineral phases link lherzolites with different textures. Most fertile lherzolites are those with protogranular textures corresponding to low degree of deformation. Secondary protogranular harzburgites represent highly refractory material after partial melting. Subsolidus temperatures of 897–1,086 °C (T_{BKN} in Table 2) inferred from the coexistence between mineral phases do not vary systematically with types of textures. Oxygen fugacity ranges from −1,03 to +0,16 log unit relative to FMQ (TB in Table 2). Harzburgites and secondary porphyroclastic xenoliths are relatively reduced with fO_2 below FMQ. Mantle in southern Slovakia belongs to moderately reduced subcontinental mantle types, showing no significant oxidation due to metasomatism or subduction process. Oxygen fugacity is in agreement with that evaluated from primary fluid inclusions (Huraiová and Konečný 1994; Konečný et al. 1995). Supposed geothermal gradient is higher by about 100 °C than the recent one calculated by 2-D forward modelling, which might be indicative of thermal subsidence. New geophysical results and re-interpretations did not prove a local mantle diapir. Geometry of Moho, lithospheric thickness, distribution of heat flow, supposed occurrence of denser rocks in the lower crust, significant vertical and horizontal stratification of rheologically different masses indicate a complicated tectonic evolution, which has to be precised.

References

BABUŠKA V., PLOMEROVÁ J. and ŠÍLENÝ J. 1987. Structural model of the subcrustal lithosphere in Central Europe. In: K.Fuchs and C. Froidevaux (Eds.), *Composition, Structure and Evolution of the Lithosphere–Asthenosphere System*, AGU Geodyn. Ser., 16, 239–251.

BALLAHAUS C., BERRY R. F. and GREEN D. H. 1991. High pressure experimental calibration of olivine–orthopyroxene–spinel oxygen geobarometer: implications for the oxidation state of the upper mantle. *Contrib. Mineral. Petrol.*, 107, 27–40.

BODNÁR J. and POSPÍŠIL L. 1980. *Geofyzikálne indície diapirizmu v neogénnych bazénoch.* MS, Geofond, Bratislava.

BONATTI E. and MICHAEL J. 1989. Mantle peridotites from continental rifts to ocean basins to subduction zones. *Earth Planet. Sci. Lett.*, 91, 297–311.

BREY G. P. and KÖHLER T. 1990. Geothermobarometry in four-phase lherzolites II. New thermobarometers, practical assessment of existing thermobarometers. *J. Petrol.*, 31, 1353–1378.

BRYNDZIA L. T. and WOOD B. J. 1990. Oxygen thermobarometry of abyssal spinel peridotites: the redox state and C-O-H volatile composition of the Earth's suboceanic upper mantle. *Am. J. Sci.*, 290, 1093–1116.

DICK H. J. B. and FISHER R. L. 1984. Mineralogical studies of residues of mantle melting: abyssal and alpine-type peridotites. In KORNPROBST J. (ed.): *Kimberlites*, 295–308. *Elsevier Press*, New York.

DOWNES H., EMBEY-ISZTIN A. and THIRLWALL M. 1992. Petrology and geochemistry of spinel peridotite xenoliths from western Pannonian Basin (Hungary): evidence for an association between enrichment and texture in the upper mantle. *Contrib. Mineral. Petrol.*, 109, 340–354.

EMBEY-ISZTIN A., SCHARBERT H. G., DIETRICH H. and POULTIDIS H. 1989. Petrology and geochemistry of peridotite xenoliths in alkali basalts from Transdanubian Volcanic region, Western Hungary. *J. Petrol.*, 30, 79–105.

FREY F. A. and PRINZ M. 1978. Ultramafic inclusions from San Carlos, Arizona: Petrologic and geochemical data bearing on their petrogenesis. *Earth Planet. Sci. Lett.*, 38, 129–176.

FUSÁN O., BIELY A., IBRMAJER J., PLANČÁR J. and ROZLOŽNÍK L. 1987. *Podložie terciéru vnútorných Západných Karpát.* GÚDŠ Bratislava, 123 pp.

GRECULA P. and VARGA I. 1979. Main discontinuity belts an the inner side of the Western Carpathians. *Miner. Slovaca*, 11, 389–403.

HORVÁTH F. 1993. Towards mechanical model for the formation of the Pannonian basin. *Tectonophysics*, 226, 333–357.

HOVORKA D. and FEJDI P. 1987. Spinel peridotite xenoliths in the West Carpathian late Cenozoic alkali basalts and their tectonic significance. *Bull. Volcanol.*, 43, 95–107.

HURAIOVÁ M. and KONEČNÝ P. 1994. Pressure–temperature conditions and oxidation state of upper mantle in the southern Slovakia. *Acta Geol. Hung.*, 37 (1–2), 33–44.

HURAIOVÁ M., DUBESSY J. and KONEČNÝ P. 1991. Composition and oxidation state of upper mantle fluids from southern Slovakia. In: ECROFI XI, *Abstracts, Plinius*, 5, 110–111.

KURAT G., EMBEY-ISZTIN A., KRACHER A. and SCHARBERT H. 1991. The upper mantle beneath Kapfenstein and the Transdanubian volcanic region. E. Austria and W. Hungary: a comparison. *Mineral. Petrol.*, 44, 21–38.

KUBOVICS I., ÁRGYELÁN G. B., SZABÓ Cs. and SOLYMOS K. G. 1988. Geochemical investigation of olivines from alkali basalt and their xenoliths (Nógrád–Gömör region, Hungary). *Acta Mineral. Petrogr. (Szeged)*, 29, 35–46.

KONEČNÝ P., KONEČNÝ V., LEXA J. and HURAIOVÁ M. 1995. Mantle xenoliths in alkali basalts of Southern Slovakia. *Acta Vulcanol.*, 7 (2), 241–247.

KÖHLER T. P. and BREY G. P. 1990. Calcium exchange between olivine and clinopyroxene calibrated as geothermobarometer for natural peridotites from 2 to 60 kb with applications. *Geochim. Cosmochim. Acta*, 54, 2375–2388.

LANKREIJER A., BIELIK M., CLOETINGH S. and MAJCIN D. 1999. Rheology predictions across the Western Carpathians, Bohemian Massif and the Pannonian Basin: implications for tectonic scenarios. *Tectonics*, (in press).

LEXA J. and KONEČNÝ V. 1979. Relationship of the Carpathian volcanic arc to the geodynamic evolution of the Pannonian Basin. In BABUŠKA V. and PALONČÁR (eds.): *Geodynamic Investigations in Czechoslovakia*, 231–235. *Veda*, Bratislava.

MAJCIN D., DUDÁŠOVÁ V. and TSVYASCHENKO V.A.1998. Tectonics and temperature field along the Carpathian profile 2T. *Contrib. Geophys. Geod.*, 28/2, 107–114.

MEDARIS L. G. and SYADA G. 1998. Spinel peridotite xenoliths from the Al Ashaer volcano, Syria: A contribution to elemental composition and thermal state of subcontinental Arabian lithosphere. *Int. Geol. Review,* 40, 305–324.

MERCIER J. C. and NICOLAS A. 1975. Textures and fabrics of upper-mantle peridotites as illustrated by xenoliths from basalts. *J. Petrol.*, 16, 454–487.

NELL J. 1989. High temperature cation distributions and thermohdynamic properties of $(Fe^{2+},Mg)(Fe^{3+},Al,Cr)_2O_4$ spinels. Ph.D. Thesis in WOODLAND A. B., KORNPROBST J. and WOOD B. J. 1992. Oxygen thermobarometry of orogenic lherzolite massifs. *J. Petrol.*, 331 , 203–230.

NICOLAS A., LUCAZEAU F. and BAYER R. 1987. Peridotite xenoliths in Massif Central, France: textural and geophysical evidence for astenopheric diapirism. In NIXON P.H. (ed.): *Mantle Xenoliths*, 563–573. *J. Wiley and Sons.*

O'REILLY S. Y. and GRIFFIN W. L. 1984. A xenolith derived geotherm for southeastern Australia and its geophysical implications. *Tectonophysics,* 111,41–64.

ROYDEN L. H., HORVÁTH F. and BURCHFIEL B.C. 1982. Transform faulting, extension, and subduction in Carphatian Pannonian region. *Geol. Soc. Amer. Bull.*, 93, 717–725.

SALTERS V. J. M., HART S. R. and PANTO Gy. 1988. Origin of late Cenozoic volcanic rocks of the Carpathian Arc, Hungary. *American Association of Petroleum Geologists, Memoir* 45, 279–292.

SIENA F. and COLTORTI M. 1993. Thermobarometric evolution and metasomatic processes of upper mantle in different tectonic settings: evidence from spinel peridotite xenoliths. *Eur. J. Mineral.*, 5, 1073–1090.

STEGENA L., GÉCZY B. and HORVÁTH F. 1975. Late Cenozoic evolution of the Pannonian basin. *Tectonophysics,* 26, 71–90.

SZABÓ Cs. and VASELLI O. 1989. Textural features and classification of ultramaphic xenoliths from Sitke (Little Plain, Hungary). *Acta Mineral. Petrol. (Szeged),* 30, 69–79.

SZALAIOVÁ V. and ŠANTAVÝ J. 1997. *Mapa úplných Bouguerových anomálií.* MS, Geocomplex, a.s. Bratislava.

ŠEFARA J., BIELIK M., KONEČNÝ P., BEZÁK V. and HURAI V. 1996. The latest stage of development of the Lithosphere and its interaction with the astenosphere (Western Carpathians). *Geol. Carpath.*, 47, 339–347.

ŠEFARA J., BIELIK M., BODNÁR J., ČÍŽEK P., FILO M., GNOJEK I., GRECULA P., HALMEŠOVÁ, S., HUSÁK Ľ., JANOŠTÍK M., KRÁL M., KUBEŠ P., KURKIN M., LEŠKO B., MIKUŠKA J., MUŠKA P., OBERNAUER D., POSPÍŠIL L., PUTIŠ M., ŠUTORA A. and VELICH 1987. *Štruktúrno-tektonická mapa prognóz nerastných surovín gefyzikálne interpretácie. Vysvetlivky k súboru máp.* MS, 267 pp.

VASELLI O., DOWNES H., THIRLWALL M., DOBOSI G., CORADOSSI N., SEGHEDI I., SZAKACS A. and VANNUCCI R. 1995. Ultramafic xenoliths in Plio-Pleistocene alkali basalts from Eastern Transylvanian Basin: Depleted mantle enriched by vein metasomatism. *J. Petrol.*, 36 (1), 23–53.

WALTER M. J. and PRESNALL D. C. 1993. Melting behavior of simplified lherzolite in the system $CaO–MgO–Al_2O_3–SiO_2$ from 7 to 35 kbar. *J. Petrol.*, 35, 329–359.

WEBB S. A. C. and WOOD B. J. 1986. Spinel–pyroxene–garnet relationships and their dependence on Cr-Al ratio. *Contrib. Mineral. Petrol.*, 92, 471–480.

WENDLANDT F. R., and MYSEN B. 1980. Melting phase relations of natural peridotite + CO_2 as a function of degree of partial melting at 15 and 30 kbar. *Amer. Mineralogist,* 65, 37–44.

WITT-EICKSCHEN G. and SECK H. A. 1991. Solubility of Ca and Al in orthopyroxene from spinel peridotite: An improved version of an empirical geothermometer. *Contrib. Mineral. Petrol.*, 106, 431–439.

WITT-EICKSCHEN G. 1993. Upper mantle xenoliths from alkali basalts of the Vogelsberg, Germany: implications for mantle upwelling and metasomatism. *Eur. J. Mineral.*, 5, 361–376.

WOOD B. J. and VIRGO D. 1989. Upper Mantle Oxidation State: Ferric iron contents of lherzolite spinels by ^{57}Fe Mössbauer spectroscopy and resultant oxygen fugacities. *Geochim. Cosmochim. Acta,* 53, 1277–1291.

WOODLAND A. B., KORNPROBST J. and WOOD B. J. 1992. Oxygen thermobarometry of orogenic lherzolite massifs. *J. Petrol.*, 331, 203–230.